S1P activates store-operated calcium entry via receptor- and non-receptor-mediated pathways in vascular smooth muscle cells

Kristen Park Hopson, Jessica Truelove, Jerold Chun, Yumei Wang and Christian Waeber

Am J Physiol Cell Physiol 300:C919-C926, 2011. First published 26 January 2011;
doi:10.1152/ajpcell.00350.2010

Am J Physiol Cell Physiol 300: C919–C926, 2011.
First published January 26, 2011; doi:10.1152/ajpcell.00350.2010.

S1P activates store-operated calcium entry via receptor- and non-receptor-mediated pathways in vascular smooth muscle cells

Kristen Park Hopson,[1] Jessica Truelove,[1] Jerold Chun,[2] Yumei Wang,[1] and Christian Waeber[1]

[1]*Stroke and Neurovascular Regulation Laboratory, Department of Radiology, Massachusetts General Hospital, Harvard Medical School, Charlestown, Massachusetts; and* [2]*Department of Molecular Biology, The Scripps Research Institute, La Jolla, California*

Submitted 30 August 2010; accepted in final form 24 January 2011

Hopson KP, Truelove J, Chun J, Wang Y, Waeber C. S1P activates store-operated calcium entry via receptor- and non-receptor-mediated pathways in vascular smooth muscle cells. *Am J Physiol Cell Physiol* 300: C919–C926, 2011. First published January 26, 2011; doi:10.1152/ajpcell.00350.2010.—Sphingosine-1-phosphate (S1P) has been shown to modulate intracellular Ca^{2+} through both G protein-coupled receptors and intracellular second messenger pathways. The precise mechanism by which S1P activates store-operated calcium entry (SOCE) in vascular smooth muscle cells (VSMCs) has not been fully characterized. Because sphingolipids and Ca^{2+} modulate proliferation and constriction in VSMCs, characterizing the connection between S1P and SOCE may provide novel therapeutic targets for vascular diseases. We found that S1P triggered STIM1 puncta formation and SOCE in VSMCs. S1P-activated SOCE was inhibited by 2-aminoethoxydiphenyl borate (2-APB), diethylstilbestrol (DES), and gadolinium (Gd^{3+}). SOCE was observed in VSMCs lacking either $S1P_2$ or $S1P_3$ receptors, suggesting that S1P acts via multiple signaling pathways. Indeed, both extracellular and intracellular S1P application increased the total internal reflection fluorescence signal in VSMCs cells transfected with STIM1-yellow fluorescent protein in a 2-APB-sensitive manner. These data, and the fact that 2-APB, DES, and Gd^{3+} all inhibited S1P-induced cerebral artery constriction, suggest that SOCE modulates S1P-induced vasoconstriction in vivo. Finally, S1P-induced SOCE was larger in proliferative than in contractile VSMCs, correlating with increases in STIM1, Orai1, $S1P_1$, and $S1P_3$ receptor mRNA. These data demonstrate that S1P can act through both receptors and a novel intracellular pathway to activate SOCE. Because S1P-induced SOCE contributes to vessel constriction and is increased in proliferative VSMCs, it is likely that S1P/SOCE signaling in proliferative VSMCs may play a role in vascular dysfunction such as atherosclerosis and diabetes.

sphingosine-1-phosphate; STIM1; sphingosine-1-phosphate receptor; blood vessels

SPHINGOSINE-1-PHOSPHATE (S1P) is an important signaling molecule in the cardiovascular system (50). S1P constricts cerebral arteries at physiologically relevant concentrations (6, 43, 48) but induces only weak vasoconstriction in peripheral vessels such as renal and coronary arteries (29, 43). The mechanism for the differences in responses to S1P in different vascular beds has not been elucidated, though differences in S1P receptor levels are thought to play a role (6). S1P is known to signal through both G protein-coupled receptor pathways ($S1P_1$–$S1P_5$) (2, 42, 50) and intracellular mechanisms (16, 24, 45) to modulate intracellular Ca^{2+} levels. Signal transduction pathways activating Ca^{2+} entry are known to be cell specific (4, 44), and although S1P has been shown to modulate intracellular Ca^{2+} stores in various cell types, it is important to examine the specific mechanisms by which S1P activates Ca^{2+} entry in vascular smooth muscle cells (VSMCs). The S1P receptors mediating Ca^{2+} signaling in VSMCs belong mainly to the $S1P_2$ and $S1P_3$ subtypes (50), but possible direct intracellular effects of S1P in these cells have not been investigated. Both genetic (42) and pharmacologic (28) inhibition of the $S1P_3$ receptor inhibit constriction of cerebral vessels. $S1P_2$ receptor null mice have normal blood pressure but exhibit decreased contractile responsiveness to α-adrenergic stimulation and resting vascular tone (22), and inhibition of $S1P_2$ has been shown to inhibit constriction of gracilis muscle resistance arteries and spiral modiolar arteries to S1P (18, 31). While this provides valuable information on the initial step of the signaling cascade that results in vessel constriction, the precise mechanism by which S1P triggers Ca^{2+} entry in VSMCs and constriction of cerebral arteries is not known.

Store-operated calcium entry (SOCE) is triggered by loss of Ca^{2+} from intracellular stores and results in activation of cation-permeable plasma membrane channels in excitable cells (for review see Refs. 20 and 36). The primary role of SOCE is to maintain Ca^{2+} levels in the endoplasmic reticulum. The mechanism has also been implicated in altering gene expression, contractility, proliferation, and migration of a variety of cells including VSMCs and endothelial cells (1, 20, 30). Depletion of Ca^{2+} from the stores causes the protein STIM1 (mainly localized to the tubular endoplasmic reticulum) to oligomerize into punctate structures within close proximity to the plasma membrane. The plasma membrane channel Orai1 is recruited to the STIM1 puncta, and the COOH terminus of STIM1 interacts with Orai1, forming active channels permeable to cations (56). Agonist stimulation of VSMCs has been shown to trigger SOCE and constrict cerebral arteries (21, 30, 33, 41).

We hypothesized that S1P triggers SOCE in VSMCs by activating STIM1 and that this pathway plays a role in vessel constriction and pathological VSMC proliferation. From our data, we conclude that S1P activates SOCE in VSMCs; S1P can act extracellularly through S1P receptors or intracellularly to trigger STIM1 puncta formation and SOCE. We found increased S1P-induced SOCE in proliferative VSMCs, which correlated with increased expression levels of relevant genes. These findings suggest that S1P-induced SOCE signaling may play a role in vascular diseases associated with proliferation.

EXPERIMENTAL PROCEDURES

Materials. S1P (Avanti Polar Lipids, Alabaster, AL) was solubilized as a millimolar stock solution in a buffer containing 100 mM Tris, 145 mM NaCl, and 4 mg/ml fatty acid-free BSA, pH 9.0, for

Address for reprint requests and other correspondence: C. Waeber, Massachusetts General Hospital, CNY149 Rm. 6403, 149 13th St., Charlestown MA 02129 (e-mail: waeber@helix.mgh.harvard.edu).

vessel experiments. For cell culture studies, S1P was added to a methanol:water (95:5) mixture in a glass vial, heated, and sonicated. When in solution, the remaining solvent was removed using a stream of nitrogen. A 1 mM S1P stock was prepared in 4 mg/ml fatty acid-free BSA. All other pharmacologic agents were purchased from Sigma (Sigma-Aldrich, St. Louis, MO) unless noted otherwise.

Animals and isolation of aortic VSMCs. All procedures were performed in accordance with the *Guide for the Care and Use of Laboratory Animals*, published by the National Institutes of Health (NIH Publication No. 85-23, Revised 1996), and were approved by the Institutional Animal Care and Use Committee. $S1P_2$ and $S1P_3$ receptor null mice (54) were bred and housed in our animal facility. Animals had free access to water and food. All experiments were performed using 20–25 g male mice, and C57BL/6 mice (Charles River Laboratories) were used for wild-type controls. Aortas were dissected from the animal and placed in ice-cold PBS, where they were cleaned of connective tissue and opened lengthwise, and endothelial cells were removed with a cotton swab. The aorta was then placed in 0.5 mg/ml elastase- 2.0 mg/ml collagenase DMEM in the incubator; cells were dispersed at 15-min intervals until all tissue was dissociated. Digestion medium containing VSMCs was spun down at 500 *g* for 10 min, supernatant was removed, and cells were resuspended in complete media and plated on appropriate dishes for the desired experiment. To obtain contractile VSMCs, cells were grown for 2 days in 0.1% FBS-DMEM (supplemented with 200 U/ml penicillin, 0.2 mg/ml streptomycin). To obtain proliferative VSMCs, cells were grown for 7 days in 1.0% FBS-DMEM. All culture reagents were obtained from GIBCO (Invitrogen). Smooth muscle cell phenotype was confirmed by staining with anti α-smooth muscle (α-SMC) actin (39): contractile VSMCs showed strong staining and retained a spindle-like shape (Supplemental Fig. S1*A*; Supplemental Material for this article is available online at the Journal website). Proliferative VSMCs expressed very little α-SMC actin, and their morphology had changed to that of proliferative SMCs (Supplemental Fig. S1*B*).

Functional studies in cerebral arteries. Adult male C57BL/6 mice were anesthetized using chloroform and killed by decapitation. The brain was removed and placed in a dissection dish filled with cold physiologic salt solution (PSS; composition in mM: 141 NaCl, 4.6 KCl, 1.7 $MgSO_4$, 0.51 EDTA, 2.7 $CaCl_2$, 10.0 HEPES, 1.1 KH_2PO_4, 4.9 glucose; pH 7.4). Posterior cerebral arteries were dissected free from connective tissue. A first-order segment of the posterior cerebral artery was cannulated, pressurized, and mounted in an arteriograph (Living Systems Instrumentation, Burlington, VT) that contained PSS (37°C, pH 7.4) for 30-min equilibration. The arterial diameter was recorded using the Video Dimension analysis system, and transmural pressure was measured and controlled using a pressure servomechanism. Pressure was produced by a peristaltic pump linked to the cannula via silicone tubing and measured using an inline transducer (Living Systems Instrumentation). Pressure was set at 60 mmHg for all experiments.

Transfection and imaging of VSMCs and COS-7 cells. For total internal reflection fluorescence (TIRF) imaging, cells were grown in glass-bottom dishes (Mattek, Ashland, MA) coated with collagen. Cells were transfected with STIM1-yellow fluorescent protein (STIM1-YFP; gift from Dr. Meyers, Stanford, CA) using lipofectamine LTX reagent (Invitrogen). Cells were imaged 24–36 h after transfection in a 37°C chamber in PSS (PSS composition in mM: 140 NaCl, 10 HEPES, 1.0 $MgCl_2$ 0.1 EGTA, 2.0 $CaCl_2$, pH 7.4). Calloway et al. (5) only observed limited STIM1 puncta formation after antigen stimulation of the IgE-receptor when compared with thapsigargin (TG)-induced puncta formation; they hypothesized that this was due to the inhibitory effect of TG on sarco(endo)plasmic reticulum Ca^{2+}-ATPase that is not imposed with the antigen, and used cytocholasin D (2 μM) and Gd^{3+} (6 μM) to improve detection of STIM1 puncta; we have used these conditions to allow for detection of STIM1 puncta formation after S1P application. TIRF imaging was performed at 37°C on a Nikon Eclipse TEi inverted epifluorescence microscope equipped with a ×60 TIRF oil immersion objective with 1.49 numerical aperture and Andor iXON EMCCD Camera (South Bridgewater, CT), and images were taken every 10 s. YFP-labeled STIM1 was excited using a C-FI TIRF filter and 40MW argon ion laser 488–514. Caged-S1P (Alexis Biochemicals, Plymouth Meeting, PA) was dissolved in DMSO to make a 10 mM stock. This solution was further diluted to 100 μM in 1 mg/ml fatty acid-free BSA. Cells were loaded with caged-S1P at concentrations noted in text in DMEM at 37°C for 30 min. Photolysis was performed by a 6-s UV pulse at maximal intensity (400dclp filter cube, Chroma Technology, Bellows Falls, VT). Images were acquired and analyzed using NIS elements (Nikon) by subtracting background intensity and then expressing data as change compared with baseline intensity.

Analysis of gene expression by real-time PCR. Total RNA extraction of mouse tissues or primary VSMCs was performed using the RNAspin Mini kit (GE Healthcare) according to the manufacturer's protocol. cDNA was synthesized from total RNA using Super-ScriptIII reverse transcriptase. Real-time PCR reactions were completed in triplicate using an ABI Prism 7000 from Applied Biosystems (Foster City, CA) with 100 ng/ml cDNA aliquots as template, together with primers and probes for STIM1, Orai1–3, $S1P_{1-3}$, and 18S ribosomal RNA (used to normalize mRNA expression). Prevalidated primers and probes were from Applied Biosystems. The gene expression data were analyzed using Qgene, a publicly available Excel script (27).

Calcium measurements. VSMCs were loaded with 5 μM Fura-2AM or Fluo-4 calcium indicator dye (Molecular Probes, Invitrogen) for 45 min and washed for 15 min in serum-free DMEM. VSMCs were stimulated with S1P (1 μM) or TG (5 μM) in 0 Ca^{2+} PSS (composition in mM: 140 NaCl, 10 HEPES, 0.09 $MgCl_2$, 0.1 EGTA). Inhibitors were added at concentrations indicated, and Ca^{2+} (2 mM) was added to measure store-operated calcium influx. For Fura-2AM experiments, VSMCs were examined with an inverted microscope (Eclipse TE200-U; Nikon, Tokyo, Japan) equipped with an Epi-Fl attachment (Nikon) and CoolSpan ER monochromator (Roper Scientific, Tucson, AZ). Image processing software (Photomatrix, HDRsoft, Montpellier, France) was used to acquire images that were taken every 8 s, monitored online, and analyzed with IPLab 3.7 software (Scanalytics, Rockville, MD). Intracellular calcium concentration ($[Ca^{2+}]_i$) was measured fluorometrically as absorbance of ratio at 340 and 380 nm ($\Delta F_{340}/F_{380}$), with 510 nm emission. For Fluo-4 experiments, VSMCs were examined with a Nikon Eclipse TEi inverted epifluorescence microscope (Nikon, Melville, NY) equipped with a ×60 oil immersion objective with 1.49 numerical aperture and Andor iXON EMCCD Camera. Fluo-4 was excited at 488 nm, and emission was recorded at 510 nm; images were taken every second. Intracellular $[Ca^{2+}]_i$ was quantified using NIS elements.

Statistical analysis. The data were analyzed with the Student's *t*-test when comparing means between two groups. $P < 0.05$ was considered statistically significant.

RESULTS

S1P induces SOCE in VSMCs. S1P modulates Ca^{2+} in VSMCs (53) and constricts brain arteries (42, 43, 48), but the precise mechanism involved in this process is not known. To test the hypothesis that S1P is acting through SOCE to induce Ca^{2+} entry and cause vessel constriction, we examined S1P-induced SOCE in primary aortic VSMCs. We first characterized pharmacologically the Ca^{2+} response in primary VSMCs (Fig. 1*A*), using three widely accepted SOCE inhibitors to assess the role of SOCE in S1P-induced Ca^{2+} entry: diethylstilbestrol (DES) (10, 55), 2-aminoethoxydiphenylborate (2-APB) (13, 26, 30, 59), and Gd^{3+} (10, 14, 49). S1P induced a large increase in SOCE when Ca^{2+} was added to the bath that was not observed when vehicle was applied followed by Ca^{2+} readdition. As seen in Fig. 1*B*, 1 μM and 10 μM DES inhibited

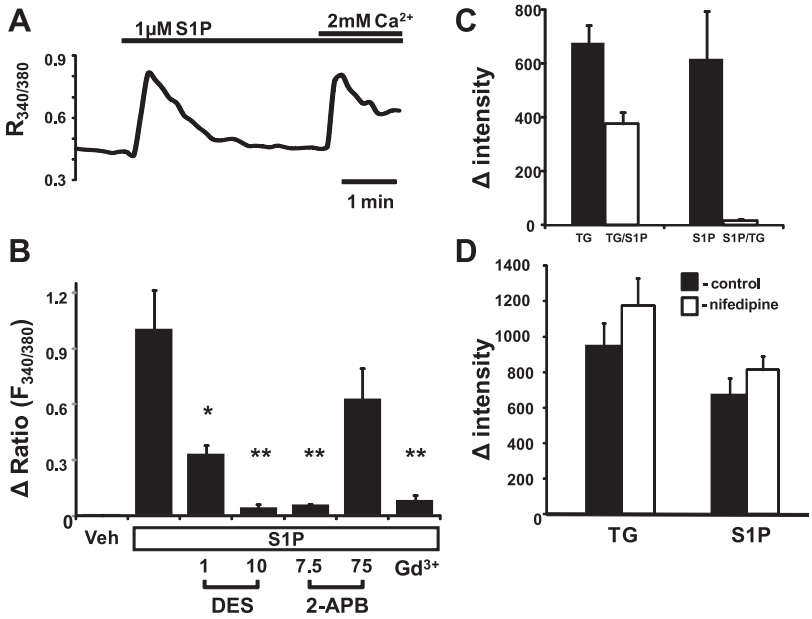

Fig. 1. Sphingosine-1-phosphate (S1P) induces store-operated calcium entry in vascular smooth muscle cells (VSMCs). *A*: representative trace of changes in Fura ratio (*R*) in VSMCs treated with S1P, followed by addition of Ca^{2+}. *B*: summary data of inhibitory effects of diethylstilbestrol (DES; 1 and 10 μM), 2-aminoethoxydiphenyl borate (2-APB; 7.5 and 75 μM), and gadolinium (Gd^{3+}; 6 μM). Veh, vehicle. *C*: S1P (1 μM) application after thapsigargin (S1P/TG, 5 μM) does not result in a further increase in intracellular calcium concentration ($[Ca^{2+}]_i$), whereas TG application after S1P-induced Ca^{2+} release (TG/S1P) does cause further increase in $[Ca^{2+}]_i$. *D*: inhibition of L-type Ca^{2+} channels by 1 μM nifedipine does not reduce TG- or S1P-induced store-operated calcium entry (SOCE). Averages represent $n = 17–28$ cells per experiment from 3 individual experiments. $*P < 0.05$, $**P < 0.01$.

this Ca^{2+} entry by 67% and 96%, respectively. Gd^{3+} (6 μM) application inhibited S1P-induced SOCE by 93%. Of note, the lower concentration (7.5 μM) of 2-APB caused a 95% inhibition of SOCE, but the higher concentration (75 μM) inhibited the Ca^{2+} entry by only 38%. Figure 1*C* demonstrates that application of S1P following depletion of stores with TG does not result in further release of Ca^{2+} from stores, whereas S1P-induced release of Ca^{2+} from the stores does not fully deplete stores because subsequent application of TG does result in a further increase in $[Ca^{2+}]_i$. Nifedipine had no effect on either TG- or S1P-induced calcium entry (Fig. 1*D*).

Both extra- and intracellular S1P trigger STIM1 puncta formation. $S1P_2$ and $S1P_3$ have been shown to contribute to vasoconstriction (18, 22, 28, 31, 42). We therefore studied S1P-induced SOCE in VSMCs prepared from aortas of $S1P_2$ and $S1P_3$ receptor-knockout mice. As expected, the initial Ca^{2+} release caused by S1P application was significantly reduced in both the $S1P_2$ and $S1P_3$ null aortic VSMCs (Fig. 2, *A* and *C*). However, S1P-induced SOCE was the same in both receptor knockouts and wild-type VSMCs (Fig. 2, *B* and *D*). To examine the role of the $S1P_1$ receptor in S1P-induced Ca^{2+} release and SOCE, we used VPC23019, an antagonist of the $S1P_1$ receptor, with limited ability (about 30-fold less) to block $S1P_3$ receptors; these experiments were therefore performed in $S1P_3^{-/-}$ VSMCs to specifically examine $S1P_1$ inhibition. S1P-induced Ca^{2+} release was completely absent when $S1P_1$ and $S1P_3$ receptors were blocked and knocked out, respectively (Fig. 2*E*), but S1P-induced SOCE remained intact (Fig. 2*F*).

Given that S1P-induced SOCE was intact in both $S1P_2$ and $S1P_3$ receptor-null VSMCs and when $S1P_1$ was inhibited, we hypothesized that S1P was able to activate SOCE in a receptor-independent manner. We performed TIRF microscopy on VSMCs transfected with STIM1-YFP (a representative trace is shown in Fig. 3*A*). Application of extracellular S1P triggered an increase in STIM1-YFP that was comparable to that caused by TG application (Fig. 3*B*). We then loaded the cells with a photolyzable (caged) derivative of S1P (24, 38) to test the effect of intracellular S1P on STIM1 localization. A 6-s exposure to UV light resulted in an increase in STIM1-YFP TIRF after photolysis of caged S1P (Fig. 3*B*). Both extracellular and intracellular S1P as well as TG-induced increases in STIM1-YFP TIRF were strongly inhibited by 2-APB (75 μM, Fig. 3*B*) (9). Similar experiments were performed in COS-7 cells, and both intracellular and extracellular application of S1P triggered increases in TIRF of STIM1-YFP (supplemental Fig. S2).

SOCE contributes to S1P-induced constriction in isolated vessels. To examine the potential functional significance of S1P-induced SOCE in VSMCs, the effect of pharmacological SOCE inhibition was examined on S1P-induced constriction of the posterior cerebral artery. 2-APB dose dependently inhibited S1P-induced constrictions (7.5 and 75 μM, Fig. 4*A*). Gd^{3+} (100 μM) (14, 40) and DES (10 μM) both significantly inhibited S1P-induced constriction as well. Interestingly, 2-APB also inhibited phenylephrine-induced constriction but had no effect on the constriction caused by the thromboxane A_2 receptor agonist U46619 (1 μM), indicating that SOCE mediates constriction to some, but not other, constrictors (supplemental Fig. S3).

Cerebral arteries constrict to S1P, whereas aorta does not (43). However, our Ca^{2+} imaging experiments performed in VSMCs from aortic cells show that S1P induces SOCE in these cells. To examine whether different levels of STIM1, Orai, and S1P receptor expression might underlie the different response of cerebral arteries vs. aorta, we performed quantitative RT-PCR in freshly isolated arteries. STIM1 expression was 5.4-fold higher in cerebral arteries than in the aorta, and both Orai2 and Orai3 expression was higher in cerebral arteries, 2.9- and 2.4-fold, respectively (Fig. 4). Expression levels of $S1P_3$ and $S1P_1$ receptors were 27-fold and 12-fold higher in cerebral vessels than aortas, respectively (Fig. 4). $S1P_2$ receptor expression was 3-fold higher in cerebral versus aortic tissue.

S1P-induced SOCE is increased in proliferative VSMCs. SOCE is known to be altered when VSMCs switch from a contractile to a proliferative phenotype (3, 32). To test the hypothesis that S1P-induced SOCE might differ in contractile

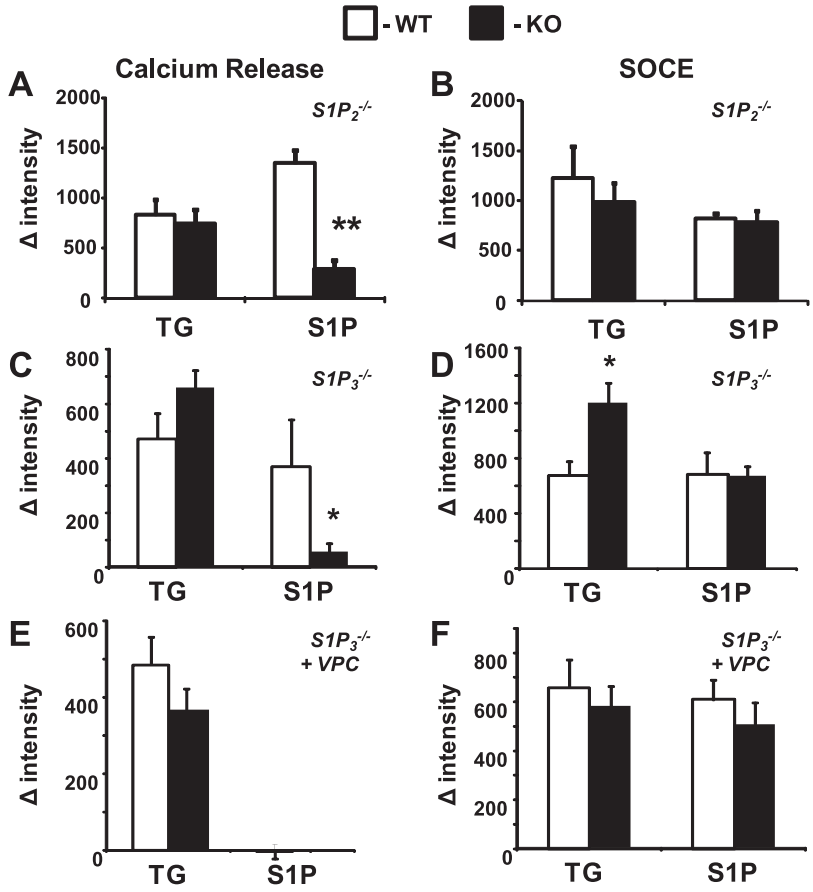

Fig. 2. S1P-induced SOCE is intact when S1P receptors are genetically absent and pharmacologically inhibited in mouse aortic VSMCs. VSMCs were cultured from $S1P_2$ and $S1P_3$ receptor-knockout mice (KO), and SOCE in response to TG (5 μM) and S1P (1 μM) was measured. *A* and *B*: the initial calcium peak was first measured after application of TG or S1P in $S1P_2^{-/-}$ VSMCs (*A*), and SOCE was measured after addition of 2 mM Ca^{2+} in response to the two drugs (*B*). *C* and *D*: the initial calcium peak was then measured in $S1P_3^{-/-}$ VSMCs after application of TG or S1P (*C*), and SOCE was measured after addition of 2 mM Ca^{2+} in response to the two drugs (*D*). *E* and *F*: finally, we used $S1P_3^{-/-}$ VSMCs treated with VPC23019 (10 μM, 30 min) to measure the initial calcium peak after application of TG or S1P (*E*) and SOCE after addition of 2 mM Ca^{2+} in response to the two drugs (*F*). WT, wild type. Averages represent $n = 10–34$ cells from 3 individual experiments. $*P < 0.05$, $**P < 0.01$.

and proliferative VSMCs, we selected culture conditions to obtain either phenotype. VSMCs grown for 2 days in 0.1% FBS showed high α-smooth muscle actin staining and retained a spindle-like structure, whereas VSMCs grown for 7 days in 1.0% FBS showed very low α-smooth muscle actin staining and displayed a more fibroblast-like morphology (supplemental results, Fig. S1). While S1P-induced SOCE was significantly smaller than TG-induced SOCE in contractile VSMCs, both agents induced similar (and higher) SOCE responses in proliferative VSMCs (Fig. 5*A*).

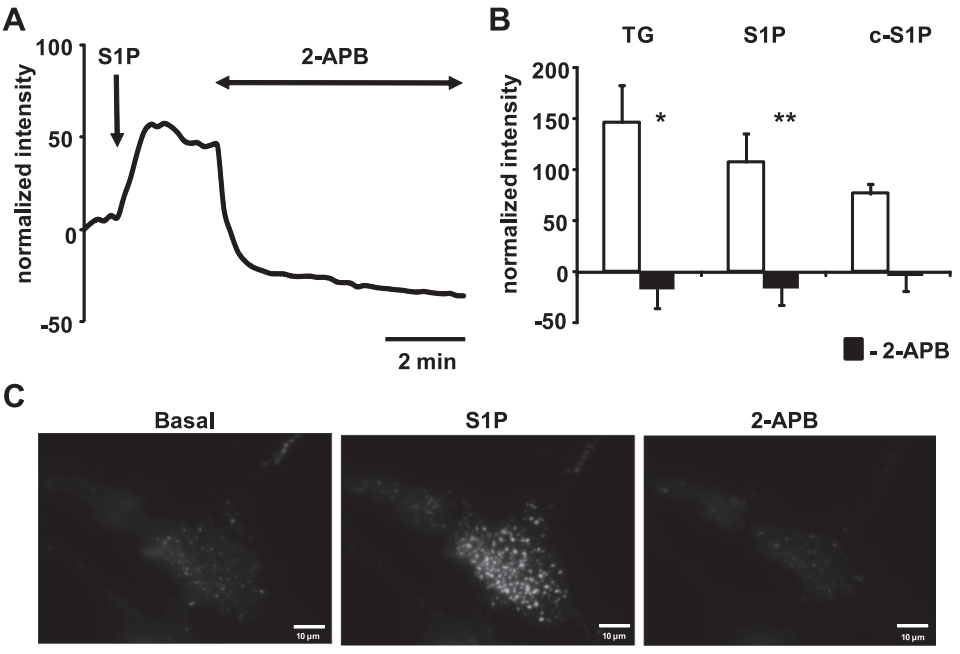

Fig. 3. Extracellular and intracellular S1P applications induce formation of STIM1-yellow fluorescent protein (YFP) puncta. VSMCs were transfected with STIM1-YFP. *A*: representative trace of total internal reflection fluorescence (TIRF) of STIM1-YFP. S1P (1 μM) application was followed by addition of 2-APB (75 μM). *B*: average increase in intensity and decrease after 2-APB application: stimulated (time $t = 180$ s) minus basal ($t = 0$) is shown for each condition [TG, 5 μM; S1P, 1 μM; caged-S1P (c-S1P), 1 μM]. *C*: representative images of STIM1-YFP puncta formation triggered by extracellular S1P (1 μM) application as seen in TIRF images; 2-APB (75 μM) reverses the accumulation of STIM1 at the plasma membrane. Cells were stimulated at $t = 30$ s with either extracellular application of TG or S1P, or a 6-s UV flash to uncage S1P. Averages represent $n = 4–15$ cells from 3 individual experiments. $*P < 0.05$, $**P < 0.01$.

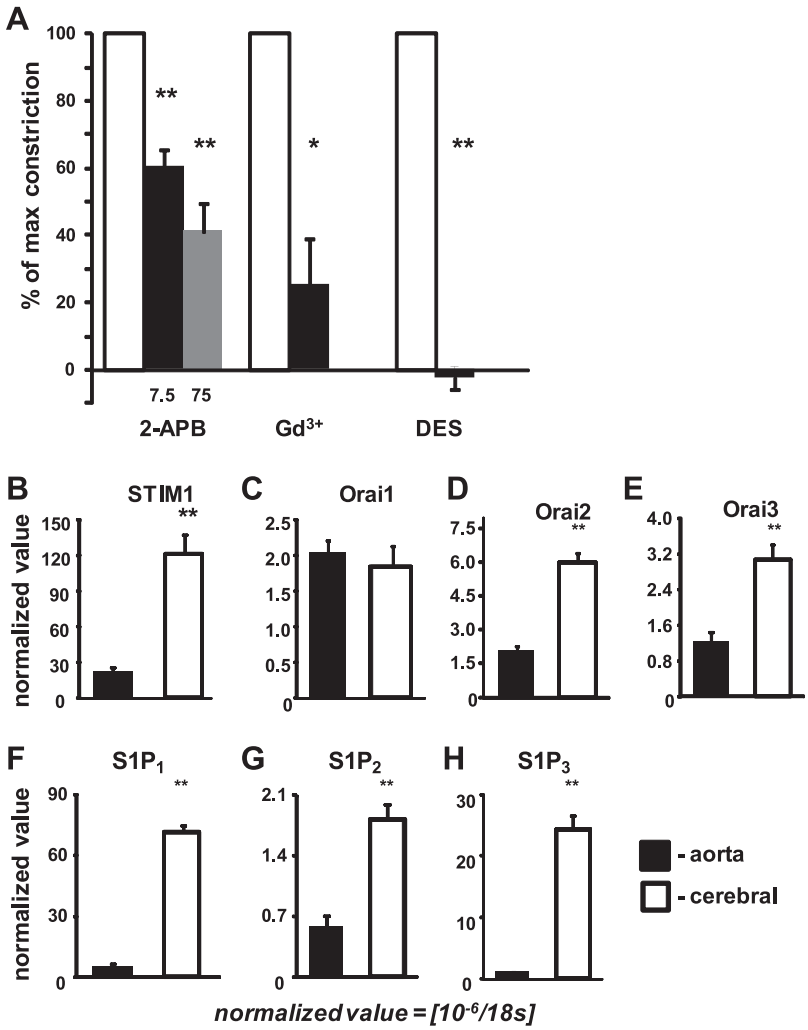

Fig. 4. S1P-induced constriction of cerebral arteries is dependent on SOCE, and STIM1, Orai, and S1P receptor gene are expressed at higher levels in cerebral arteries than aorta. A posterior cerebral artery was mounted in an intact vessel arteriograph. *A*: vessels were constricted with S1P (1 μM), and 2-APB (7.5 and 75 μM), Gd^{3+} (100 μM), or DES (10 μM) was applied on top of the stable constriction. Averages represent $n = 3–8$ vessels from individual animals. mRNA levels were measured using quantitative RT-PCR (*B–H*). Averages represent $n = 6$ individual experiments. $*P < 0.05$, $**P < 0.01$.

Because increased STIM1 and Orai1 levels have been reported to coincide with VSMC switch from a contractile to a proliferative phenotype and associated SOCE alterations (32), we next examined whether the increased SOCE in response to S1P in proliferative VSMCs was associated with altered expression of STIM1 and Orai (Fig. 5). STIM1 expression was significantly increased (2.6-fold) in primary aortic VSMCs grown under proliferative conditions compared with those grown under contractile conditions. Orai1 and Orai2 expression was also increased (1.8- and 2-fold, respectively) in VSMCs grown under proliferative conditions. Because the increased S1P-induced SOCE response in proliferative VSMCs suggested S1P receptor upregulation, we compared the expression levels of the three S1P receptors potentially involved in VSMC signaling (17, 50): $S1P_1$ (4.9-fold) and $S1P_3$ (2.3-fold) receptor expression were both significantly increased in VSMCs grown in proliferative culture conditions (Fig. 5). Expression of $S1P_2$ receptor was not significantly different between the two culture conditions.

DISCUSSION

This study shows that S1P can act through receptor-dependent or -independent mechanisms to activate STIM1 and SOCE in vascular smooth muscle cells. We found that this pathway contributes to constriction of cerebral arteries and is upregulated in proliferative VSMCs. These findings emphasize the physiologic relevance of this pathway and suggest a novel signaling mechanism for potential therapeutic intervention in vascular disease associated with VSMC proliferation.

We observed S1P-induced STIM1 puncta formation using TIRF microscopy, indicating that S1P can trigger activation of SOCE. While puncta formation has been documented in cells lines using thapsigargin (36), our observation is important because it is made in primary VSMCs, using an agent, S1P, known to play a major role in the cardiovascular system under both physiological (6) and pathological conditions (11, 15). Although S1P has been shown to modulate intracellular Ca^{2+} stores in VSMCs (6, 8, 23), this is the first pharmacological characterization of S1P-induced Ca^{2+} entry and of direct intracellular effects of S1P in these cells. Our direct observation of STIM1 activation in VSMCs is important because STIM1 is now known to be involved in other processes than Ca^{2+} signaling (19). Three inhibitors of SOCE (2-APB, DES, Gd^{3+}) blocked S1P-induced Ca^{2+} entry in primary VSMCs. Although these inhibitors can have nonspecific effects, they are routinely used to study

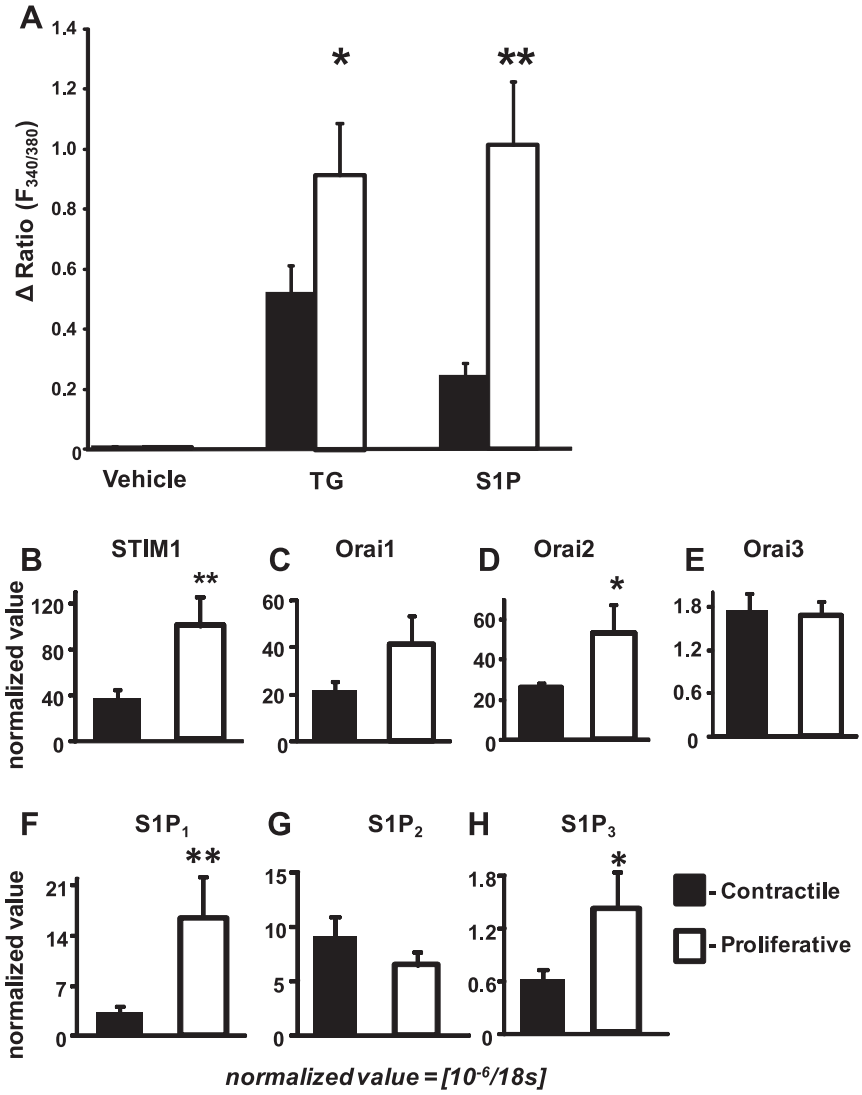

Fig. 5. TG- and S1P-induced SOCE, and gene expression in contractile and proliferative VSMCs. Primary cultures of aortic VSMCs were grown under either proliferative (0.1% FBS for 2 days) or contractile (1.0% FBS for 7 days) conditions, and SOCE was measured in response to TG (5 μM) or S1P (1 μM) (*A*). Averages represent n = 21–42 cells per experiment from 3 individual experiments. mRNA levels were measured using quantitative RT-PCR (*B–H*). Averages of $n = 8$ and $n = 7$ are shown for 0.1% FBS and 1.0% FBS experiments, respectively. $^*P < 0.05$, $^{**}P < 0.01$.

SOCE (as reviewed in Refs. 10, 13, 20, and 37). Because there is still debate in the literature on the coupling of STIM1 with TRPC and Orai channel, further experiments are needed to definitely show whether STIM1 only associated with Orai in VSMCs to trigger SOCE. The finding that 2-APB significantly inhibited S1P-induced SOCE at low (7.5 μM), but not at high, concentrations (75 μM) could reflect the known ability of 2-APB to activate Orai3 channels at higher (50 μM) concentrations (9, 59). Our data in primary VSMC demonstrate that 2-APB can completely reverse STIM1 puncta formation. Similar findings have been published by other laboratories, and it is hypothesized that 2-APB not only has direct actions on channel inhibition but also uncouples STIM1 from Orai and reverses STIM1 oligomerization (9, 47). S1P-induced puncta formation of STIM1, taken together with the consistent effect of three different inhibitors, strongly indicates that S1P activates SOCE in VSMCs. Our data are in agreement with the literature demonstrating a role for SOCE in refilling Ca^{2+} stores in VSMCs and in the regulation of vascular reactivity (30, 46, 52, 56, 58).

As extensively documented, $S1P_{1–3}$ are expressed in VSMCs while $S1P_4$ and $S1P_5$ are absent (for review see Ref. 25). Although signaling through $S1P_2$ and $S1P_3$ receptors has been shown to contribute to S1P-induced vasoconstriction (22, 42, 43), the present results obtained in $S1P_2$ and $S1P_3$ receptor-null aortic VSMCs and in VSMCs in which $S1P_1$ was inhibited with VPC23019 demonstrate that S1P can signal either via other receptors or via intracellular mechanisms to induce SOCE. To test this hypothesis, we used a previously characterized photolyzable S1P derivative to release S1P inside VSMCs (24). Caged S1P has been shown to release Ca^{2+} from endoplasmic reticulum Ca^{2+} stores (24), but downstream SOCE activation has not been reported. Here we show that caged S1P activates SOCE by visualizing STIM1 recruitment to the plasma membrane. It might be argued that S1P generated from photolysis of intracellular caged S1P might leech out and activate G protein-coupled receptor, but this possibility was ruled out in a previous study using caged S1P (24). Therefore our results strongly suggest that intracellular S1P can activate SOCE. The exact mechanisms of this novel signaling pathway have yet to be characterized.

We then set out to highlight the physiologic relevance of this pathway under physiological (cerebral vessel constriction) and potentially pathological conditions (VSMC proliferation). The functional significance of primary culture data was established in intact vessels by demonstrating the inhibition of S1P-induced constriction of the posterior cerebral artery by 2-APB, Gd^{3+}, and DES. While inhibition by 2-APB of phenylephrine-induced cerebral artery constrictions has been previously reported (30), the lack of effect of 2-APB on thromboxane A_2 receptor-induced constriction (U46619) suggests possible differences in the signaling pathways of S1P (or phenylephrine) and thromboxane A_2 and their differential ability to activate SOCE.

S1P-induced SOCE was demonstrated in aortic VSMCs, and the posterior cerebral artery was used to assess the role of SOCE in S1P-induced vessel constriction; we hypothesized that differences in expression patterns of STIM1, Orais, and S1P receptors in the two vascular beds could explain why cerebral vessels constrict to S1P while aorta does not. S1P receptor expression studies have been previously compared in different vessels (6), leading to the suggestion that higher expression of S1P receptors in cerebral arteries could account for the fact that S1P elicits a much stronger constriction in cerebral arteries than in the aorta. Based on our finding that all components of the SOCE pathway except Orai1 are more highly expressed in cerebral arteries than in aorta, and S1P receptors are more highly expressed in the cerebral vessels as well, we hypothesize that differential expression of proteins of the SOCE pathway might also play a key role in the vessel specific constriction to S1P.

VSMC proliferation is a critical component of vascular dysfunction such as diabetes and atherosclerosis. Because SOCE is upregulated in proliferative VSMCs (32), we hypothesized that S1P-induced SOCE might be specifically upregulated in proliferative VSMCs, which was indeed the case. The finding of increased SOCE in response to S1P is particularly interesting in light of proliferative vascular diseases in which S1P is known to play a role (6, 7). It is tempting to speculate that STIM1 and Orai upregulation is the cause of the increase in SOCE that we see in proliferative VSMCs. In addition, proliferative VSMCs also showed increased expression of S1P receptor mRNAs. This may explain why S1P-induced SOCE was comparable to that of TG-induced SOCE in proliferative VSMCs, while both the S1P and TG responses were increased in these cells.

Emphasizing the relevance of our findings to proliferative VSMC diseases, changes in S1P receptors in response to acute balloon injury were found in the rat carotid artery, leading to the conclusion that $S1P_1$/$S1P_3$ receptors promote proliferation (51). Dysregulation of SOCE has been implicated in diabetes, atherosclerosis and hypertension (12, 14, 57) and SOCE has also been shown to phosphorylate cyclic AMP response element-binding (CREB) protein and upregulate proliferative genes (34, 35). With the new knowledge that S1P can activate SOCE and that S1P receptors, STIM1, Orais, and SOCE are all upregulated in proliferative VSMCs, it will be interesting to study the link between S1P and SOCE in proliferative vascular diseases. It is likely that inhibition of this pathway might reduce vascular dysfunction (increased contractility/proliferation) in these conditions.

ACKNOWLEDGMENTS

The authors are grateful to Dr. Tobias Meyer (Stanford University, Stanford, CA), who generously provided the STIM1-YFP construct.

GRANTS

This study was supported by National Institutes of Health Grants R01NS049263 and P01NS055104 (to C. Waeber), 5T32AG00277 (to K. P. Hopson), and DA019674 and DC009505 (to J. Chun).

DISCLOSURES

No conflicts of interest, financial or otherwise, are declared by the author(s).

REFERENCES

1. **Abdullaev IF, Bisaillon JM, Potier M, Gonzalez JC, Motiani RK, Trebak M.** Stim1 and Orai1 mediate CRAC currents and store-operated calcium entry important for endothelial cell proliferation. *Circ Res* 103: 1289–1299, 2008.
2. **Anliker B, Chun J.** Cell surface receptors in lysophospholipid signaling. *Semin Cell Dev Biol* 15: 457–465, 2004.
3. **Berra-Romani R, Mazzocco-Spezzia A, Pulina MV, Golovina VA.** Ca^{2+} handling is altered when arterial myocytes progress from a contractile to a proliferative phenotype in culture. *Am J Physiol Cell Physiol* 295: C779–C790, 2008.
4. **Bootman MD, Berridge MJ, Roderick HL.** Calcium signalling: more messengers, more channels, more complexity. *Curr Biol* 12: R563–R565, 2002.
5. **Calloway N, Vig M, Kinet JP, Holowka D, Baird B.** Molecular clustering of STIM1 with Orai1/CRACM1 at the plasma membrane depends dynamically on depletion of Ca^{2+} stores and on electrostatic interactions. *Mol Biol Cell* 20: 389–399, 2009.
6. **Coussin F, Scott RH, Wise A, Nixon GF.** Comparison of sphingosine 1-phosphate-induced intracellular signaling pathways in vascular smooth muscles: differential role in vasoconstriction. *Circ Res* 91: 151–157, 2002.
7. **Daum G, Grabski A, Reidy MA.** Sphingosine 1-phosphate: a regulator of arterial lesions. *Arterioscler Thromb Vasc Biol* 29: 1439–1443, 2009.
8. **David KC, Scott RH, Nixon GF.** Advanced glycation endproducts induce a proliferative response in vascular smooth muscle cells via altered calcium signaling. *Biochem Pharmacol* 76: 1110–1120, 2008.
9. **DeHaven WI, Smyth JT, Boyles RR, Bird GS, Putney JW Jr.** Complex actions of 2-aminoethyldiphenyl borate on store-operated calcium entry. *J Biol Chem* 283: 19265–19273, 2008.
10. **Derler I, Fritsch R, Schindl R, Romanin C.** CRAC inhibitors: identification and potential. *Expert Opin Drug Discov* 3: 787–800, 2008.
11. **Deutschman DH, Carstens JS, Klepper RL, Smith WS, Page MT, Young TR, Gleason LA, Nakajima N, Sabbadini RA.** Predicting obstructive coronary artery disease with serum sphingosine-1-phosphate. *Am Heart J* 146: 62–68, 2003.
12. **Fellner SK, Arendshorst WJ.** Store-operated Ca^{2+} entry is exaggerated in fresh preglomerular vascular smooth muscle cells of SHR. *Kidney Int* 61: 2132–2141, 2002.
13. **Flemming R, Xu SZ, Beech DJ.** Pharmacological profile of store-operated channels in cerebral arteriolar smooth muscle cells. *Br J Pharmacol* 139: 955–965, 2003.
14. **Giachini FR, Chiao CW, Carneiro FS, Lima VV, Carneiro ZN, Dorrance AM, Tostes RC, Webb RC.** Increased activation of stromal interaction molecule-1/Orai-1 in aorta from hypertensive rats: a novel insight into vascular dysfunction. *Hypertension* 53: 409–416, 2009.
15. **Grabski AD, Shimizu T, Deou J, Mahoney WM Jr, Reidy MA, Daum G.** Sphingosine-1-phosphate receptor-2 regulates expression of smooth muscle alpha-actin after arterial injury. *Arterioscler Thromb Vasc Biol* 29: 1644–1650, 2009.
16. **Hla T.** Signaling and biological actions of sphingosine 1-phosphate. *Pharm Res* 47: 401–407, 2003.
17. **Ishii I, Ye X, Friedman B, Kawamura S, Contos JJ, Kingsbury MA, Yang AH, Zhang G, Brown JH, Chun J.** Marked perinatal lethality and cellular signaling deficits in mice null for the two sphingosine 1-phosphate (S1P) receptors, $S1P_2$/LP_{B2}/EDG-5 and $S1P_3$/LP_{B3}/EDG-3. *J Biol Chem* 277: 25152–25159, 2002.
18. **Kono M, Belyantseva IA, Skoura A, Frolenkov GI, Starost MF, Dreier JL, Lidington D, Bolz SS, Friedman TB, Hla T, Proia RL.** Deafness and stria vascularis defects in $S1P_2$ receptor-null mice. *J Biol Chem* 282: 10690–10696, 2007.

19. **Lefkimmiatis K, Srikanthan M, Maiellaro I, Moyer MP, Curci S, Hofer AM.** Store-operated cyclic AMP signalling mediated by STIM1. *Nat Cell Biol* 11: 433–442, 2009.
20. **Leung FP, Yung LM, Yao X, Laher I, Huang Y.** Store-operated calcium entry in vascular smooth muscle. *Br J Pharmacol* 153: 846–857, 2008.
21. **Liou J, Kim ML, Heo WD, Jones JT, Myers JW, Ferrell JE Jr, Meyer T.** STIM is a Ca^{2+} sensor essential for Ca^{2+}-store-depletion-triggered Ca^{2+} influx. *Curr Biol* 15: 1235–1241, 2005.
22. **Lorenz JN, Arend LJ, Robitz R, Paul RJ, MacLennan AJ.** Vascular dysfunction in $S1P_2$ sphingosine 1-phosphate receptor knockout mice. *Am J Physiol Regul Integr Comp Physiol* 292: R440–R446, 2007.
23. **Mathieson FA, Nixon GF.** Sphingolipids differentially regulate mitogen-activated protein kinases and intracellular Ca^{2+} in vascular smooth muscle: effects on CREB activation. *Br J Pharmacol* 147: 351–359, 2006.
24. **Meyer zu Heringdorf D, Liliom K, Schaefer M, Danneberg K, Jaggar JH, Tigyi G, Jakobs KH.** Photolysis of intracellular caged sphingosine-1-phosphate causes Ca^{2+} mobilization independently of G-protein-coupled receptors. *FEBS Lett* 554: 443–449, 2003.
25. **Michel MC, Mulders AC, Jongsma M, Alewijnse AE, Peters SL.** Vascular effects of sphingolipids. *Acta Paediatr Suppl* 96: 44–48, 2007.
26. **Muik M, Fahrner M, Derler I, Schindl R, Bergsmann J, Frischauf I, Groschner K, Romanin C.** A cytosolic homomerization and a modulatory domain within STIM1 C terminus determine coupling to ORAI1 channels. *J Biol Chem* 284: 8421–8426, 2009.
27. **Muller PY, Janovjak H, Miserez AR, Dobbie Z.** Processing of gene expression data generated by quantitative real-time RT-PCR. *Biotechniques* 32: 1372–1374, 1376.
28. **Murakami A, Takasugi H, Ohnuma S, Koide Y, Sakurai A, Takeda S, Hasegawa T, Sasamori J, Konno T, Hayashi K, Watanabe Y, Mori K, Sato Y, Takahashi A, Mochizuki N, Takakura N.** Sphingosine 1-phosphate (S1P) regulates vascular contraction via $S1P_3$ receptor: investigation based on a new $S1P_3$ receptor antagonist. *Mol Pharmacol* 77: 704–713, 2010.
29. **Ohmori T, Yatomi Y, Osada M, Kazama F, Takafuta T, Ikeda H, Ozaki Y.** Sphingosine 1-phosphate induces contraction of coronary artery smooth muscle cells via $S1P_2$. *Cardiovasc Res* 58: 170–177, 2003.
30. **Park KM, Trucillo M, Serban N, Cohen RA, Bolotina VM.** Role of iPLA2 and store-operated channels in agonist-induced Ca^{2+} influx and constriction in cerebral, mesenteric, and carotid arteries. *Am J Physiol Heart Circ Physiol* 294: H1183–H1187, 2008.
31. **Peter BF, Lidington D, Harada A, Bolz HJ, Vogel L, Heximer S, Spiegel S, Pohl U, Bolz SS.** Role of sphingosine-1-phosphate phosphohydrolase 1 in the regulation of resistance artery tone. *Circ Res* 103: 315–324, 2008.
32. **Potier M, Gonzalez JC, Motiani RK, Abdullaev IF, Bisaillon JM, Singer HA, Trebak M.** Evidence for STIM1- and Orai1-dependent store-operated calcium influx through ICRAC in vascular smooth muscle cells: role in proliferation and migration. *FASEB J* 23: 2425–2437, 2009.
33. **Prakriya M, Feske S, Gwack Y, Srikanth S, Rao A, Hogan PG.** Orai1 is an essential pore subunit of the CRAC channel. *Nature* 443: 230–233, 2006.
34. **Pulver-Kaste RA, Barlow CA, Bond J, Watson A, Penar PL, Tranmer B, Lounsbury KM.** Ca^{2+} source-dependent transcription of CRE-containing genes in vascular smooth muscle. *Am J Physiol Heart Circ Physiol* 291: H97–H105, 2006.
35. **Pulver RA, Rose-Curtis P, Roe MW, Wellman GC, Lounsbury KM.** Store-operated Ca^{2+} entry activates the CREB transcription factor in vascular smooth muscle. *Circ Res* 94: 1351–1358, 2004.
36. **Putney JW.** Capacitative calcium entry: from concept to molecules. *Immunol Rev* 231: 10–22, 2009.
37. **Putney JW Jr.** Pharmacology of capacitative calcium entry. *Mol Interv* 1: 84–94, 2001.
38. **Qiao L, Kozikowski AP, Olivera A, Spiegel S.** Synthesis and evaluation of a photolyzable derivative of sphingosine 1-phosphate–caged SPP. *Bioorg Med Chem Lett* 8: 711–714, 1998.
39. **Rensen SS, Doevendans PA, van Eys GJ.** Regulation and characteristics of vascular smooth muscle cell phenotypic diversity. *Neth Heart J* 15: 100–108, 2007.
40. **Rodat-Despoix L, Aires V, Ducret T, Marthan R, Savineau JP, Rousseau E, Guibert C.** Signalling pathways involved in the contractile response to 5-HT in the human pulmonary artery. *Eur Respir J* 34: 1338–1347, 2009.
41. **Ross K, Whitaker M, Reynolds NJ.** Agonist-induced calcium entry correlates with STIM1 translocation. *J Cell Physiol* 211: 569–576, 2007.
42. **Salomone S, Potts EM, Tyndall S, Ip PC, Chun J, Brinkmann V, Waeber C.** Analysis of sphingosine 1-phosphate receptors involved in constriction of isolated cerebral arteries with receptor null mice and pharmacological tools. *Br J Pharmacol* 153: 140–147, 2008.
43. **Salomone S, Yoshimura S, Reuter U, Foley M, Thomas SS, Moskowitz MA, Waeber C.** $S1P_3$ receptors mediate the potent constriction of cerebral arteries by sphingosine-1-phosphate. *Eur J Pharmacol* 469: 125–134, 2003.
44. **Spiegel S, Merrill AH Jr.** Sphingolipid metabolism and cell growth regulation. *FASEB J* 10: 1388–1397, 1996.
45. **Spiegel S, Milstien S.** Sphingosine-1-phosphate: an enigmatic signalling lipid. *Nat Rev Mol Cell Biol* 4: 397–407, 2003.
46. **Takahashi Y, Watanabe H, Murakami M, Ono K, Munehisa Y, Koyama T, Nobori K, Iijima T, Ito H.** Functional role of stromal interaction molecule 1 (STIM1) in vascular smooth muscle cells. *Biochem Biophys Res Commun* 361: 934–940, 2007.
47. **Tamarina NA, Kuznetsov A, Philipson LH.** Reversible translocation of EYFP-tagged STIM1 is coupled to calcium influx in insulin secreting beta-cells. *Cell Calcium* 44: 533–544, 2008.
48. **Tosaka M, Okajima F, Hashiba Y, Saito N, Nagano T, Watanabe T, Kimura T, Sasaki T.** Sphingosine 1-phosphate contracts canine basilar arteries in vitro and in vivo: possible role in pathogenesis of cerebral vasospasm. *Stroke* 32: 2913–2919, 2001.
49. **Varnai P, Hunyady L, Balla T.** STIM and Orai: the long-awaited constituents of store-operated calcium entry. *Trends Pharmacol Sci* 30: 118–128, 2009.
50. **Waeber C, Blondeau N, Salomone S.** Vascular sphingosine-1-phosphate $S1P_1$ and $S1P_3$ receptors. *Drug News Perspect* 17: 365–382, 2004.
51. **Wamhoff BR, Lynch KR, Macdonald TL, Owens GK.** Sphingosine-1-phosphate receptor subtypes differentially regulate smooth muscle cell phenotype. *Arterioscler Thromb Vasc Biol* 28: 1454–1461, 2008.
52. **Wang S, Zhang Y, Wier WG, Yu X, Zhao M, Hu H, Sun L, He X, Wang Y, Wang B, Zang W.** Role of store-operated Ca^{2+} entry in adenosine-induced vasodilatation of rat small mesenteric artery. *Am J Physiol Heart Circ Physiol* 297: H347–H354, 2009.
53. **Watterson KR, Ratz PH, Spiegel S.** The role of sphingosine-1-phosphate in smooth muscle contraction. *Cell Signal* 17: 289–298, 2005.
54. **Yang AH, Ishii I, Chun J.** In vivo roles of lysophospholipid receptors revealed by gene targeting studies in mice. *Biochim Biophys Acta* 1582: 197–203, 2002.
55. **Zakharov SI, Smani T, Dobrydneva Y, Monje F, Fichandler C, Blackmore PF, Bolotina VM.** Diethylstilbestrol is a potent inhibitor of store-operated channels and capacitative Ca^{2+} influx. *Mol Pharmacol* 66: 702–707, 2004.
56. **Zakharov SI, Smani T, Leno E, Macianskiene R, Mubagwa K, Bolotina VM.** Monovalent cation (MC) current in cardiac and smooth muscle cells: regulation by intracellular Mg^{2+} and inhibition by polycations. *Br J Pharmacol* 138: 234–244, 2003.
57. **Zbidi H, Lopez JJ, Amor NB, Bartegi A, Salido GM, Rosado JA.** Enhanced expression of STIM1/Orai1 and TRPC3 in platelets from patients with type 2 diabetes mellitus. *Blood Cells Mol Dis* 43: 211–213, 2009.
58. **Zhang J, Wier WG, Blaustein MP.** Mg^{2+} blocks myogenic tone but not K^+-induced constriction: role for SOCs in small arteries. *Am J Physiol Heart Circ Physiol* 283: H2692–H2705, 2002.
59. **Zhang SL, Kozak JA, Jiang W, Yeromin AV, Chen J, Yu Y, Penna A, Shen W, Chi V, Cahalan MD.** Store-dependent and -independent modes regulating Ca^{2+} release-activated Ca^{2+} channel activity of human Orai1 and Orai3. *J Biol Chem* 283: 17662–17671, 2008.